

Correlations between Ca II H&K Emission and the Gaia M dwarf Gap

2 EMILY M. BOUDREAU¹, AYLIN GARCIA SOTO¹, AND BRIAN C. CHABOYER¹

3 ¹*Department of Physics and Astronomy, Dartmouth College, Hanover, NH 03755, USA*

4 (Received 02/07/2024; Revised 02/20/2024; Accepted)

5 Submitted to ApJ

6 ABSTRACT

7 The Gaia M dwarf gap, also known as the Jao Gap, is a novel feature discovered in the Gaia DR2 G vs.
8 BP-RP color magnitude diagram. This gap represents a 17 percent decrease in stellar density in a thin
9 magnitude band around the convective transition mass ($\sim 0.35M_{\odot}$) on the main sequence. Previous
10 work has demonstrated a paucity of Hydrogen Alpha emission coincident with the G magnitude of
11 the Jao Gap in the solar neighborhood. The exact mechanism which results in this paucity is as
12 of yet unknown; however, the authors of the originating paper suggest that it may be the result of
13 complex variations to a star's magnetic topology driven by the Jao Gap's characteristic formation and
14 breakdown of stars' radiative transition zones. We present a follow up investigating another widely used
15 magnetic activity metric, Calcium II H&K emission. Ca II H&K activity appears to share a similar
16 anomalous behavior as H α does near the Jao Gap magnitude. We observe an increase in star-to-star
17 variation of magnetic activity near the Jao Gap. **We present a toy model of a stars magnetic
18 field evolution which demonstrates that** this increase may be due to stochastic disruptions to
19 the magnetic field originating from the periodic mixing events characteristic of the convective kissing
20 instabilities which drive the formation of the Jao Gap.

21 *Keywords:* Stellar Evolution (1599) — Stellar Evolutionary Models (2046)

22 1. INTRODUCTION

23 The initial mass requirements of molecular clouds col-
24 lapsing to form stars results in a strong bias towards
25 lower masses and later spectral classes during star for-
26 mation. Partly as a result of this bias and partly as a
27 result of their extremely long main-sequence lifetimes, M
28 Dwarfs make up approximately 70 percent of all stars in
29 the galaxy (Winters et al. 2019). Moreover, many planet
30 search campaigns have focused on M Dwarfs due to the
31 relative ease of detecting small planets in their habitable
32 zones (e.g. Nutzman & Charbonneau 2008). M Dwarfs
33 then represent both a key component of the galactic stel-
34 lar population as well as the most numerous possible set
35 of stars which may host habitable exoplanets. Given this
36 key location M Dwarfs occupy in modern astronomy it

37 is important to have a thorough understanding of their
38 structure and evolution.

39 Jao et al. (2018) discovered a novel feature in the Gaia
40 Data Release 2 (DR2) $G_{BP} - G_{RP}$ color-magnitude-
41 diagram. Around $M_G = 10$ there is an approximately
42 17 percent decrease in stellar density of the sample of
43 stars Jao et al. (2018) considered. Subsequently, this
44 has become known as either the Jao Gap, or Gaia M
45 Dwarf Gap. Following the initial detection of the Gap
46 in DR2 the Gap has also potentially been observed in
47 2MASS (Skrutskie et al. 2006; Jao et al. 2018); however,
48 the significance of this detection is quite weak and it re-
49 lies on the prior of the Gap's location from Gaia data.
50 The Gap is also present in Gaia Early Data Release 3
51 (EDR3) (Jao & Feiden 2021). These EDR3 and 2MASS
52 data sets then indicate that this feature is not a bias
53 inherent to DR2.

54 The Gap is generally attributed to convective instabil-
55 ities in the cores of stars straddling the fully convective
56 transition mass (0.3 - 0.35 M_{\odot}) **known as convective
57 kissing instabilities** (Baraffe & Chabrier 2018). These

Corresponding author: Emily M. Boudreaux
emily.m.boudreaux.gr@dartmouth.edu,
emily@boudreauxmail.com

instabilities interrupt the normal, slow, main sequence luminosity evolution of a star and result in luminosities lower than expected from the main sequence mass-luminosity relation (Jao & Feiden 2020).

The Jao Gap, inherently a feature of M Dwarf populations, provides an enticing and unique view into the interior physics of these stars (Feiden et al. 2021). This is especially important as, unlike more massive stars, M Dwarf seismology is infeasible due to the short periods and extremely small magnitudes which both radial and low-order low-degree non-radial seismic waves are predicted to have in such low mass stars (Rodríguez-López 2019). The Jao Gap therefore provides one of the only current methods to probe the interior physics of M Dwarfs.

The magnetic activity of M dwarfs is of particular interest due to the theorised links between habitability and the magnetic environment which a planet resides within (e.g. Lammer et al. 2012; Gallet et al. 2017; Kislyakova et al. 2017). M dwarfs are known to be more magnetically active than earlier type stars (Saar & Linsky 1985; Astudillo-Defru et al. 2017; Wright et al. 2018) while simultaneously this same high activity calls into question the canonical magnetic dynamo believed to drive the magnetic field of solar-like stars (the $\alpha\Omega$ dynamo) (Shulyak et al. 2015). One primary challenge which M dwarfs pose is that stars less than approximately $0.35 M_{\odot}$ are composed of a single convective region. This denies any dynamo model differential rotation between adjacent levels within the star. Alternative dynamo models have been proposed, such as the α^2 dynamo along with modifications to the $\alpha\Omega$ dynamo which may be predictive of M dwarf magnetic fields (Chabrier & Küker 2006; Kochukhov 2021; Kleorin et al. 2023).

Despite this work, very few studies have dived specifically into the magnetic field of M dwarfs at or near the convective transition region. This is not surprising as that only spans approximately a 0.2 magnitude region in the Gaia BP-RP color magnitude diagram and is therefore populated by a relatively small sample of stars.

Jao et al. (2023) identify the Jao Gap as a strong discontinuity point for magnetic activity in M dwarfs. Two primary observations from their work are that the Gap serves as a boundary where very few active stars, in their sample of 640 M dwarfs, exist below the Gap and that the overall downward trend of activity moving to fainter magnitudes is anomalously high in within the 0.2 mag range of the Gap. Jao et al. Figures 3 and 13 make this paucity in H α emission particularly clear. Based on previous work from Spada & Lanzafame (2020); Curtis et al. (2020); Dungee et al. (2022) the authors propose that the mechanism resulting in the reduced fraction of

active stars within the Gap is that as the radiative zone dissipates due to core expansion, angular momentum from the outer convective zone is dumped into the core resulting in a faster spin down than would otherwise be possible. Effectively the core of the star acts as a sink, reducing the amount of angular momentum which needs to be lost by magnetic braking for the outer convective region to reach the same angular velocity. Given that H α emission is strongly coupled magnetic activity in the upper chromosphere (Newton et al. 2016; Kumar et al. 2023) and that a star’s angular velocity is a primary factor in its magnetic activity, a faster spin down will serve to more quickly dampen H α activity.

In addition to H α the Calcium Fraunhofer lines may be used to trace the magnetic activity of a star. These lines originate from magnetic heating of the lower chromosphere driven by magnetic shear stresses within the star. Both Perdelwitz et al. (2021) and Boudreaux et al. (2022) present calcium emission measurements for stars spanning the Jao Gap. In this paper we search for similar trends in the Ca II H& K emission as Jao et al. see in the H α emission. In Section 2 we investigate the empirical star-to-star variability in emission and quantify if this could be due to noise or sample bias; in Section 3 we present a simplified toy model which shows that the mixing events characteristic of convective kissing instabilities could lead to increased star-to-star variability in activity as is seen empirically.

2. CORRELATION

Using Ca II H&K emission data from Perdelwitz et al. (2021) and Boudreaux et al. (2022) (quantified using the R'_{HK} metric Middelkoop 1982; Rutten 1984) we investigate the correlation between the Jao Gap magnitude and stellar magnetic activity. We are more statistically limited here than past authors have been due to the requirement for high resolution spectroscopic data when measuring Calcium emission.

The merged dataset is presented in Figure 1. **The sample overlap between Perdelwitz et al. (2021) and Boudreaux et al. (2022) is small (only consisting of five targets). For those five targets there is an approximately 1.5 percent average difference between measured $\log(R'_{HK})$ values, with measurements from Boudreaux et al. biased to be slightly more negative than those from Perdelwitz et al.**

There is a visual discontinuity in the spread of stellar activity below the Jao Gap magnitude. **Further discussion of why there may be disagreement between the observed magnitude of the gap and the discontinuity which we identify may be found in**

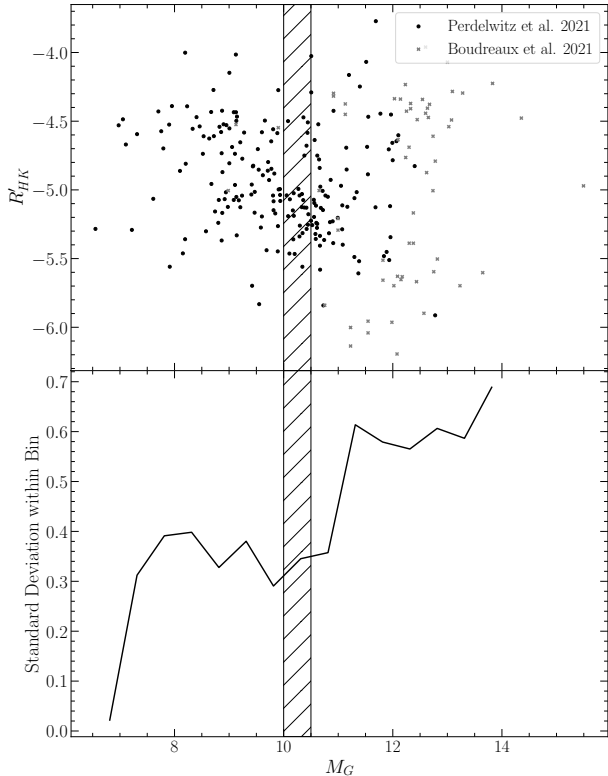


Figure 1. Merged Dataset from [Perdelwitz et al. \(2021\)](#); [Boudreaux et al. \(2022\)](#). Note the increase in the spread of R'_{HK} around the Jao Gap Magnitude (**top**). **Standard deviation of Calcium emission data within each bin. Note the discontinuity near the Jao Gap Magnitude (bottom).** The location of the Gap as identified in literature is shown by the hatched region (~ 10 - $10.5 M_G$). Potential explanations for the disagreement in magnitude are discussed in detail in [Section 2.1](#).

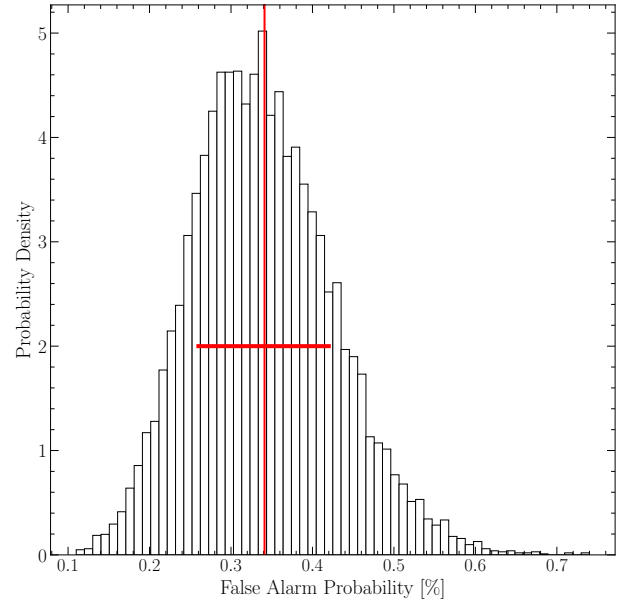


Figure 2. Probability distribution of the false alarm probability for the discontinuity seen in [Figure 1](#). The mean of this distribution is $0.341\% \pm 0.08$.

161 **Section 2.1.** In order to quantify the significance of this
 162 discontinuity we measure the false alarm probability of
 163 the change in standard deviation.

164 First we split the merged dataset into bins with a
 165 width of 0.5 mag. In each bin we measure the stan-
 166 dard deviation about the mean of the data. The results
 167 of this are shown in [Figure 1](#) (bottom). In order to mea-
 168 sure the false alarm probability of this discontinuity we
 169 first resample the merged calcium emission data based
 170 on the associated uncertainties for each datum as pre-
 171 sented in their respective publications. Then, for each
 172 of these “resample trials” we measure the probability
 173 that a change in the standard deviation of the size seen
 174 would happen purely due to noise. Results of this test
 175 are show in in [Figure 2](#).

176 This rapid increase star-to-star variability would only
 177 arise due purely to noise 0.3 ± 0.08 percent of the time
 178 and is therefore likely either a true effect or an alias of
 179 some sample bias.

180 If the observed increase in variability is not due to a
 181 sample bias and rather is a physically driven effect then
 182 there is an obvious similarity between these findings and
 183 those of [Jao et al. \(2023\)](#). Specifically we find a increase
 184 in variability below the magnitude of the Gap. More-
 185 over, this variability increase is primarily driven by an
 186 increase in the number of low activity stars (as opposed
 187 to an increase in the number of high activity stars). We
 188 can further investigate the observed change in variability
 189 for only low activity stars by filtering out those stars at
 190 or above the saturated threshold for magnetic activity.
 191 [Boudreaux et al. \(2022\)](#) identify $\log(R'_{HK}) = -4.436$
 192 as the saturation threshold. We adopt this value and
 193 filter out all stars where $\log(R'_{HK}) \geq -4.436$. Apply-
 194 ing the same analysis to this reduced dataset as was
 195 done to the full dataset we still find a discontinuity at
 196 the same location ([Figure 3](#)). This discontinuity is of a
 197 smaller magnitude and consequently is more likely to be
 198 due purely to noise, with a 7 ± 0.2 percent false alarm
 199 probability. This false alarm probability is however only
 200 concerned with the first point after the jump in vari-
 201 ability. If we consider the false alarm probability of the
 202 entire high variability region then the probability that
 203 the high variability region is due purely to noise drops
 204 to 1.4 ± 0.04 percent.

205 **Further, various authors have shown that the**
 206 **strength of Calcium II H&K emission may evolve**
 207 **over month to year timescales (e.g. [Rauscher &](#)**
 208 **[Marcy 2006](#); [Perdelwitz et al. 2021](#); [Cretignier](#)**
 209 **[et al. 2024](#)). Targets from [Boudreaux et al.](#)**

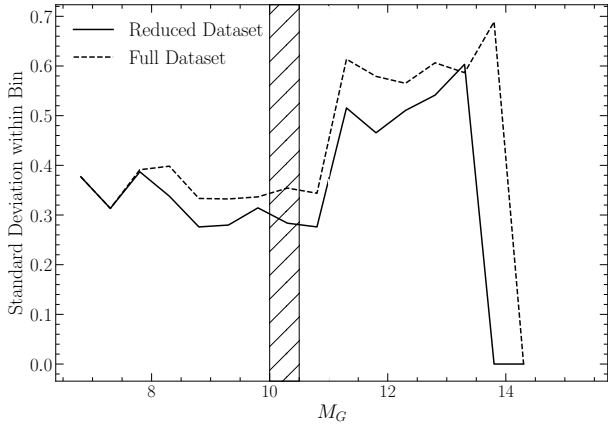


Figure 3. Spread in the magnetic activity metric for the merged sample with any stars $\log(R'_{HK}) > -4.436$ filtered out. The location of the Gap as identified in literature is shown by the hatched region ($\sim 10-10.5 M_G$).

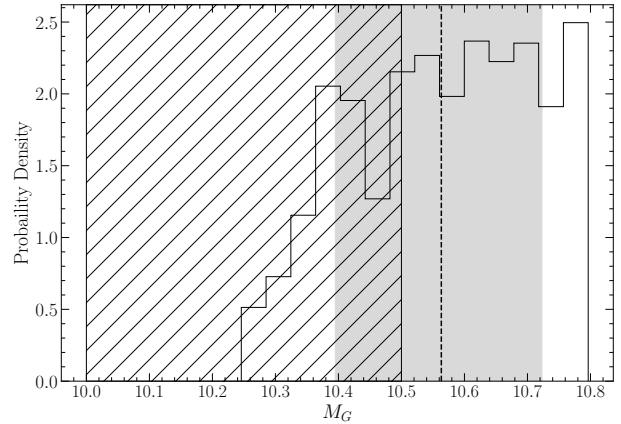


Figure 4. Probability density distribution of discontinuity location as identified in the merged dataset. The dashed line represents the mean of the distribution while the shaded region runs from the 16th percentile to the 84th percentile of the distribution. This distribution was built from 10,000 independent samples where the discontinuity was identified as the highest value in the gradient of the standard deviation. The location of the Gap as identified in literature is shown by the hatched region ($\sim 10-10.5 M_G$).

(2022) were observed an average of only four times and over year long timescales. Therefore, the nominal $\log(R'_{HK})$ values derived in that work may be biased by stellar variability. However, the scale of observed variability in the activity metric is significantly smaller than the star-to-star activity variability addressed here and therefore activity cycles are not expected to be of particular relevance. Specifically, the amplitude of variability is generally $\Delta \log(R'_{HK}) \lesssim 0.2$ whereas in this work we address variability on the order of $\Delta \log(R'_{HK}) \lesssim 2$.

We observe a strong, likely statistically significant, discontinuity in the star-to-star variability of Ca II H&K emission below the magnitude of the Jao Gap. However, modeling is required to determine if this discontinuity may be due to the same underlying physics.

2.1. Coincidence with the Jao Gap Magnitude

While the observed increase in variability seen here does not seem to be coincident with the Jao Gap — instead appearing to be approximately 0.5 mag fainter, in agreement with what is observed in Jao et al. (2023) — a number of complicating factors prevent us from falsifying that these two features are not coincident. Jao et al. find, similar to the results presented here, that the paucity of $H\alpha$ emission originates below the Gap. Moreover, we use a 0.5 magnitude bin size when measuring the star-to-star variability which injects error into the positioning of any feature in magnitude space. We can quantify the degree of uncertainty the magnitude bin choice injects by conducting Monte Carlo trials where bins are randomly shifted redder or bluer. We conduct 10,000 trials where each trial involves sampling

a random shift to the bin start location from a normal distribution with a standard deviation of 1 magnitude. For each trial we identify the discontinuity location as the maximum value of the gradient of the standard deviation (this is the derivative of the data in Figures ?? & 3). Some trials result in the maximal value lying at the 0th index of the magnitude array due to edge effects, these trials are rejected (and account for 11% of the trials). The uncertainty in the identified magnitude of the discontinuity due to the selected start point of the magnitude bins reveals a $1\sigma = \pm 0.32$ magnitude uncertainty in the location of the discontinuity (Figure 4). Finally, all previous studies of the M dwarf Gap (Jao et al. 2018; Jao & Feiden 2021; Mansfield & Kroupa 2021; Boudreaux et al. 2022; Jao et al. 2023) demonstrate that the Gap has a color dependency, shifting to fainter magnitudes as the population reddens and consequently an exact magnitude range is ill-defined. Therefore we cannot falsify the model that the discontinuity in star-to-star activity variability is coincident with the Jao Gap magnitude.

2.2. Rotation

It is well known that star's magnetic activity tend to be correlated with their rotational velocity (Vaughan et al. 1981; Newton et al. 2016; Astudillo-Defru et al. 2017; Houdebine et al. 2017; Boudreaux et al. 2022); therefore, we investigate whether there is a similar correlation between Gap location and rotational period in our dataset. All targets from Boudreaux et al. (2022)

272 already have published rotational periods; however, tar-
 273 gets from [Perdelwitz et al. \(2021\)](#) do not necessarily have
 274 published periods. Therefore, we derive photometric ro-
 275 tational periods for these targets here. Given the in-
 276 herent heterogeneity of M Dwarf stellar surfaces ([Boisse
 277 et al. 2011; Robertson et al. 2020](#)) we are able to deter-
 278 mine the rotational period of a star through the anal-
 279 ysis of active regions. Various methodologies can be
 280 employed for this purpose, including the examination of
 281 photometry and light curves (e.g., [Newton et al. 2016](#)),
 282 and the observation of temporal changes in the strength
 283 of chromospheric emission lines such as Ca II H & K
 284 or H α (e.g., [Fuhrmeister et al. 2019; Kumar & Fares
 285 2023](#)). In this work, new rotational periods are derived
 286 from TESS 2-minute cadence data¹.

287 Due to both the large frequency and amplitudes of
 288 M dwarf flaring rates the photometric period can prove
 289 difficult to measure — as frequency directly correlates
 290 with periodicity. Thus, following the process described
 291 in [García Soto et al. \(2023\)](#), we utilize two methods in
 292 this paper to reduce the effect of flares. One method
 293 uses `stella` a python package which implements a series
 294 of pre-trained convolutional neural networks (CNNs) to
 295 remove flare-shaped features in a light curve ([Feinstein
 296 et al. 2020a](#)). The second method separates a star’s pho-
 297 tometry into 10 minute bins to account for misshapen
 298 flares which `stella` is known to be biased against de-
 299 tecting.

300 `stella` employs a diverse library of models trained
 301 with varying initial seeds ([Feinstein et al. 2020b,a](#)). The
 302 Convolutional Neural Networks in `stella` are trained
 303 on labeled TESS 2-min for both flares and non-flares.
 304 For the purposes of this paper, we use an ensemble
 305 of 100 models in `stella`’s library to optimize model
 306 performance ([Feinstein et al. 2020b](#), for further detail).
 307 `stella` scores flairs with a probability of between 0 to
 308 1 — where higher values indicate a higher confidence
 309 that a feature is a flare. Here we adopt a score of 0.5 as
 310 the cutoff threshold, all features with a score of 0.5 or
 311 greater are classed as flares and removed (e.g. [Feinstein
 312 et al. 2020b](#)).

313 Furthermore, we also bin the data from a 2-min to
 314 10-min cadence using the python package `lightkurve`’s
 315 binning function ([Lightkurve Collaboration et al. 2018;
 316 Barentsen et al. 2020](#)). This further reduces any flaring-
 317 contribution that might have been missed by `stella`².
 318 Subsequently, we filter photometry, only retaining data

319 whos residuals are less than 4 times the root-mean-
 320 square deviation.

321 Gaussian processes for modeling the periods are based
 322 on [Angus et al. \(2018\)](#) for the subset of M Dwarfs with
 323 no fiducial periods. The `starspot` package is adapted
 324 for light curve analysis ([Angus 2021; Angus & Gar-
 325 cia Soto 2023](#)). Our Gaussian process kernel function
 326 incorporates two stochastically-driven simple harmonic
 327 oscillators, representing primary (P_{rot}) and secondary
 328 ($P_{\text{rot}}/2$) rotation modes. First, we implement the Lomb-
 329 Scargle periodogram within `starspot` to initially esti-
 330 mate the period. After which, we create a maximum
 331 a posteriori (MAP) fit using `starspot` to generate a
 332 model for stellar rotation. To obtain the posterior of
 333 the stellar rotation model, we use Markov Chain Monte
 334 Carlo (MCMC) sampling using the `pymc3` package ([Sal-
 335 vatier et al. 2016](#)) within our adapted `starspot` version.
 336 All rotational periods are presented in Table 1. Our fi-
 337 nal sample contains 187 stars with measured rotational
 338 periods. We derive new rotational periods for 7 of these.

339 One might expect a decrease in mean rotational period
 340 around the magnitude of the Gap, due to the slight de-
 341 crease in magnetic activity. However, there is no statis-
 342 tically significant correlation between rotational period
 343 and G magnitude which we can detect given our sam-
 344 ple size (Figure 5). Rotational period is however, not
 345 the ideal parametrization to use, as magnetic activity is
 346 more directly related to the Rossby number (Ro). Us-
 347 ing the empirical calibration presented in [Wright et al.
 348 \(2018\)](#) (Equation 1) we find the mixing timescale for
 349 each star such that the Rossby Number is defined as
 350 $Ro = P_{\text{rot}}/\tau_c$.

$$\tau_c = 0.64 + 0.25 * (V - K) \quad (1)$$

351 When we compare Rossby number to G magnitude
 352 (Figure 6) we find that there may be a slight paucity
 353 of rotation coincident with the decrease in spread of the
 354 activity metric. We quantify the statistical significance
 355 of this drop by building a Gaussian kernel density esti-
 356 mator (kde) based on the data outside of this range,
 357 and then resampling that kde 10000 times for each data
 358 point in the theorized paucity range. The false alarm
 359 probability that that drop is due to noise is then the
 360 product of the fraction of samples which are less than
 361 or equal to the value of each data point. We find that
 362 there is a 0.022 percent probability that this dip is due
 363 purely to noise.

2.3. Limitations

364
 365 There are two primary limitation of our dataset. First,
 366 we only have 264 star in our dataset (with measured
 367 R'_{HK} , 187 with rotational periods) limiting the statis-

¹ Some M Dwarfs lacking a documented rotational period did not have sufficient TESS data to yield fiducial rotational periods

² This is relevant for flares that are misshapen at the start or break in the dataset due to missing either the ingress or egress.

ID	G Mag	V Mag	K Mag	$\log(R'_{HK})$	$e_Log(R'_{HK})$	Ro	prot	r_prot
	mag	mag	mag				d	
2MASS J00094508-4201396	12.14	13.659	8.223	-4.339	0.001	0.009	0.859	Bou22
2MASS J00310412-7201061	12.301	13.648	8.445	-5.388	0.003	0.928	80.969	Bou22
2MASS J01040695-6522272	12.447	13.95	8.532	-4.489	0.001	0.006	0.624	Bou22
2MASS J02004725-1021209	12.778	14.113	9.092	-4.791	0.001	0.188	14.793	Bou22
2MASS J02014384-1017295	13.026	14.477	9.189	-4.54	0.001	0.034	3.152	Bou22
2MASS J02125458+0000167	12.096	13.58	8.168	-4.635	0.001	0.048	4.732	Bou22
2MASS J02411510-0432177	12.251	13.79	8.246	-4.427	0.001	0.004	0.4	Bou22
2MASS J03100305-2341308	12.23	13.5	8.567	-4.234	0.001	0.028	2.083	Bou22
2MASS J03205178-6351524	12.087	13.433	8.195	-5.629	0.004	1.029	91.622	Bou22
2MASS J05015746-0656459	10.649	12.196	6.736	-5.005	0.002	0.875	88.5	Bou22

Table 1. First 10 rows of the dataset used in this work. This data is available as a machine readable supliment to this article.

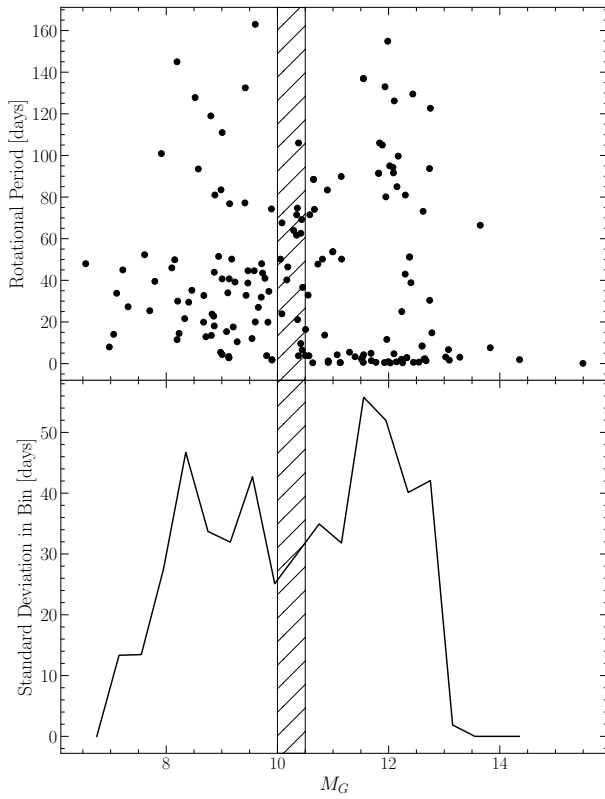


Figure 5. Rotational Periods against G magnitude for all stars with rotational periods (top). Standard deviation of rotational period within magnitude bin (bottom). **The location of the Gap as identified in literature is shown by the hatched region ($\sim 10-10.5 M_G$).**

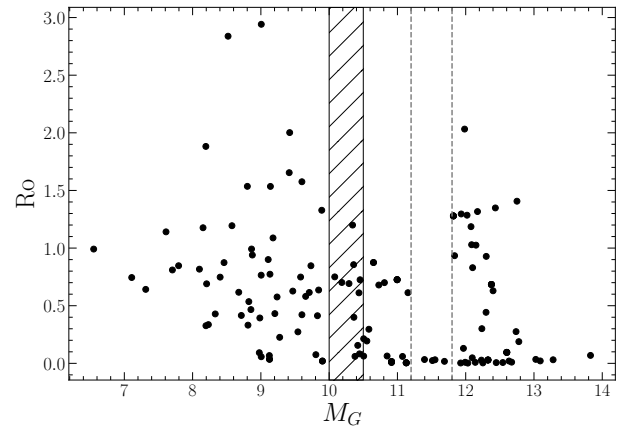


Figure 6. Rossby number vs. G magnitude for all stars with rotational periods and V-K colors on Simbad. Dashed lines represent the hypothesized region of decreased rotation. **The location of the Gap as identified in literature is shown by the hatched region ($\sim 10-10.5 M_G$).**

372 tions ($R \sim 16000$) and a comparatively blue wavelength
373 range ³.

374 Additionally, the sample we do have does not extend
375 to as low mass as would be ideal. This presents a degeneracy
376 between two potential causes for the observed increased
377 star-to-star variability. One option, as presented
378 above and elaborated on in the following section, is that
379 this is due to kissing instabilities. However, another
380 possibility is that this increased variability is intrinsic
381 to the magnetic fields of fully convective stars. This al-

368 tical power of our analysis. This is primarily due to
369 the relative difficulty of obtaining Ca II H&K measure-
370 ments compared to obtaining $H\alpha$ measurements. Re-
371 liable measurements require both high spectral resolu-

³ wrt. to what many spectrographs cover. There is no unified
resource listing currently commissioned spectrographs; however,
it is somewhat hard to source glass which transmits well at H&K
wavelengths limiting the lower wavelength of most spectrographs.

ternate option may be further supported by the shape of the magnetic activity spread vs. G magnitude relation. Convective kissing instabilities are not expected to continue to much lower masses than the fully convective transition mass. The fact that the increase in variance which we observe continues to much fainter magnitudes would therefore be somewhat surprising in a purely convective kissing instability driven framework (though the degeneracy between potentially physically driven increase in variance and increase in variance due to the noise-magnitude relation complicates attempts to constrain this.) There is limited discussion in the literature of overall magnetic field strength spanning the fully convective transition mass; however, Shulyak et al. (2019) present estimated magnetic field strengths for 47 M dwarfs, spanning a larger area around the convective transition region and their dataset does not indicate a inherently increased variability for fully convective stars.

3. MODELING

One of the most pressing questions related to this work is whether or not the increased star-to-star variability in the activity metric and the Jao Gap, which are coincident in magnitude, are driven by the same underlying mechanism. The challenge when addressing this question arises from current computational limitations. Specifically, the kinds of three dimensional magneto-hydrodynamical simulations — which would be needed to derive the effects of convective kissing instabilities on the magnetic field of the star — are infeasible to run over gigayear timescales while maintaining thermal timescale resolutions needed to resolve periodic mixing events.

In order to address this and answer the specific question of *could kissing instabilities result in increased star-to-star variability of the magnetic field*, we adopt a very simple toy model. Kissing instabilities result in a transient radiative zone separating the core of a star (convective) from its envelope (convective). When this radiative zone breaks down two important things happen: one, the entire star becomes mechanically coupled, and two, convective currents can now move over the entire radius of the star. Jao et al. (2023) propose that this mechanical coupling may allow the star’s core to act as an angular momentum sink thus accelerating a stars spin down and resulting in anomalously low H α emission.

Regardless of the exact mechanism by which the magnetic field may be affected, it is reasonable to expect that both the mechanical coupling and the change to the scale of convective currents will have some effect on the star’s magnetic field. On a microscopic scale both of these will change how packets of charge within a star move and may serve to disrupt a stable dynamo.

Therefore, in the model we present here we make only one primary assumption: *every mixing event may modify the star’s magnetic field by some amount*. Within our model this assumption manifests as a random linear perturbation applied to some base magnetic field at every mixing event. The strength of this perturbation is sampled from a normal distribution with some standard deviation, σ_B .

Synthetic stars are sampled from a grid of stellar models evolved using the Dartmouth Stellar Evolution Program (DSEP) with similar parameters to those used in Boudreaux & Chaboyer (2023). Each stellar model was evolved using a high temporal resolution (timesteps no larger than 10,000 years) and typical numerical tolerances of one part in 10^5 . Each model was based on a GS98 (Grevesse & Sauval 1998) solar composition with a mass range from 0.3 M_\odot to 0.4 M_\odot . Finally, models adopt OPLIB high temperature radiative opacities, Ferguson 2004 low temperature radiative opacities, and include both atomic diffusion and gravitational settling. A Kippenhan-Iben diagram showing the structural evolution of a model within the Gap is shown in Figure 7.

Each synthetic star is assigned some base magnetic activity ($B_0 \sim \mathcal{N}(1, \sigma_B)$) and then the number of mixing events before some age t are counted based on local maxima in the core temperature. The toy magnetic activity at age t for the model is given in Equation 2. An example of the magnetic evolution resulting from this model is given in Figure 8. Fundamentally, this model presents magnetic activity variation due to mixing events as a random walk and therefore results will increasing divergence over time.

$$B(t) = B_0 + \sum_i B_i \sim \mathcal{N}(1, \sigma_B) \quad (2)$$

Applying the same analysis to these models as was done to the observations as described in Section 2 we find that this simple model results in a qualitatively similar trend in the standard deviation vs. Magnitude graph (Figure 9). In order to reproduce the approximately 50 percent change to the spread of the activity metric observed in the combined dataset in section 2 a distribution with a standard deviation of 0.1 is required when sampling the change in the magnetic activity metric at each mixing event. This corresponds to 68 percent of mixing events modifying the activity strength by 10 percent or less. The interpretation here is important: what this qualitative similarity demonstrates is that it may be reasonable to expect kissing instabilities to result in the observed increased star-to-star variation. Importantly, we are not able to claim that kissing instabilities *do* lead

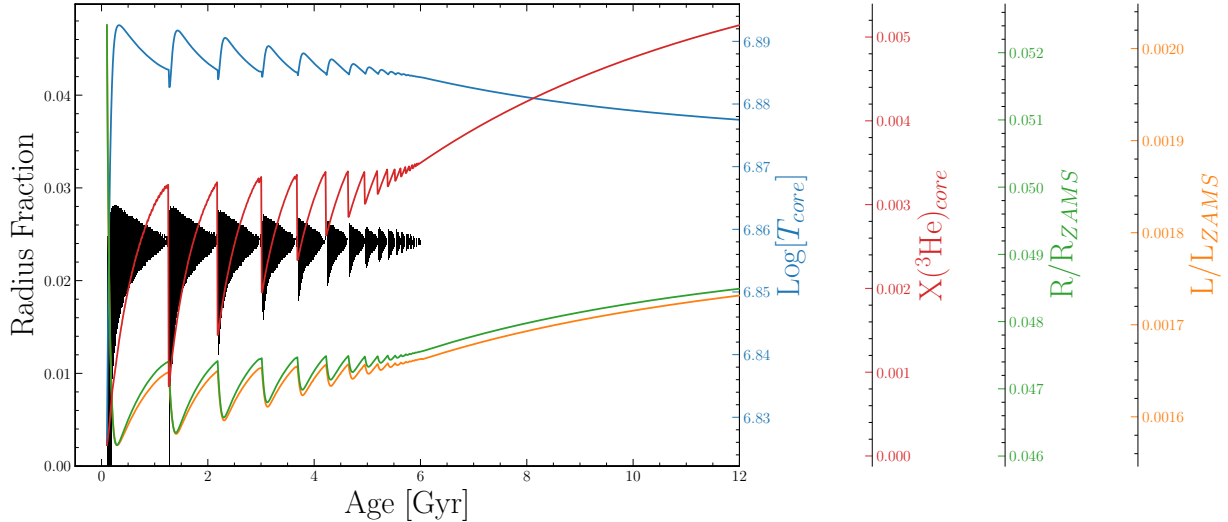


Figure 7. Kippenhan-Iben diagram for a 0.345 solar mass star. Note the periodic mixing events (where the plotted curves peak).

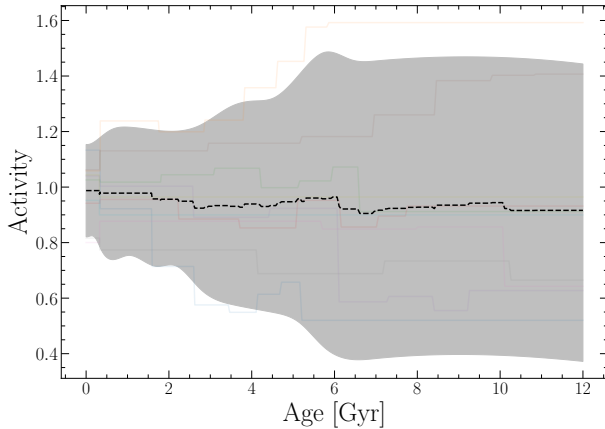


Figure 8. Example of the toy model presented here resulting in increased divergence between stars magnetic fields. The shaded region represents the maximum spread in the two point correlation function at each age.

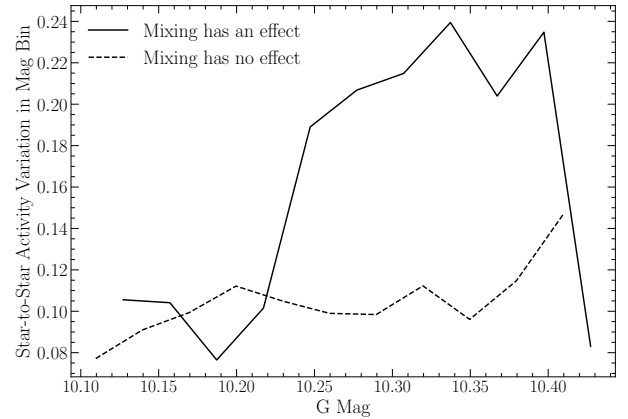


Figure 9. Toy model results showing a qualitatively similar discontinuity in the star-to-star magnetic activity variability.

482 to these increased variations, only that they reasonably
 483 could. Further modeling, observational, and theoretical
 484 efforts will be needed to more definitively answer this
 485 question.

3.1. Limitations

486
 487 The model presented in this paper is very limited and
 488 it is important to keep these limitations in mind when in-
 489 terpreting the results presented here. Some of the main
 490 challenges which should be leveled at this model are the
 491 assumption that the magnetic field will be altered by
 492 some small random perturbation at every mixing event.
 493 This assumption was informed by the large number of
 494 free parameters available to a physical star during the
 495 establishment of a large scale magnetic field and the as-

496 sociated likely stochastic nature of that process. How-
 497 ever, it is similarly believable that the magnetic field
 498 will tend to alter in a uniform manner at each mixing
 499 event. For example, since differential rotation is gener-
 500 ally proportional to the temperature gradient within a
 501 star and activity is strongly coupled to differential rota-
 502 tion then it may be that as the radiative zone reforms
 503 over thermal timescales the homogenization of angular
 504 momentum throughout the star results in overall lower
 505 amounts of differential rotation each after mixing event
 506 than would otherwise be present.

507 Moreover, this model does not consider how other de-
 508 generate sources of magnetic evolution such as stellar
 509 spin down, relaxation, or coronal heating may effect
 510 star-to-star variability. These could conceivably lead to
 511 a similar increase in star-to-star variability which is co-
 512 incident with the Jao Gap magnitude as the switch from

513 fully to partially convective may effect efficiency of these
514 process.

515 Additionally, there are challenges with this toy model
516 that originate from the stellar evolutionary model. Ob-
517 servations of the Jao Gap show that the feature is not
518 perpendicular to the magnitude axis; rather, it is in-
519 versely proportional to the color. No models of the Jao
520 Gap published at the time of writing capture this color
521 dependency and *what causes this color dependency* re-
522 mains one of the most pressing questions relating to the
523 underlying physics. This non captured physics is one
524 potential explanation for why the magnitude where our
525 model predicts the increase in variability is not in agree-
526 ment with where the variability jump exists in the data.

527 Finally, we have not considered detailed descriptions
528 of the dynamos of stars. The magnetohydrodynamical
529 modeling which would be required to model the evolu-
530 tion of the magnetic field of these stars at thermal
531 timescale resolutions over gigayears is currently beyond
532 the ability of practical computing. Therefore future
533 work should focus on limited modeling which may in-
534 form the evolution of the magnetic field directly around
535 the time of a mixing event.

536 4. CONCLUSION

537 It is, at this point, well established that the Jao Gap
538 may provide a unique view of the interiors of stars for
539 which other probes, such as seismology, fail. However, it
540 has only recently become clear that the Gap may lend
541 insight into not just structural changes within a star
542 but also into the magnetic environment of the star. *Jao*
543 *et al. (2023)* presented evidence that the physics driv-
544 ing the Gap might additionally result in a paucity of
545 H α emission. These authors propose potential physical
546 mechanisms which could explain this paucity, including
547 the core of the star acting as an angular momentum sink
548 during mixing events.

549 Here we have expanded upon this work by probing
550 the degree and variability of Calcium II H&K emission
551 around the Jao Gap. We lack the same statistical power
552 of *Jao et al.*'s sample; however, by focusing on the star-
553 to-star variability within magnitude bins we are able
554 to retain statistical power. We find that there is an
555 anomalous increase in variability at a G magnitude of
556 ~ 11 . This is only slightly below the observed mean gap
557 magnitude.

558 Additionally, we propose a simple model to explain
559 this variability. Making the assumption that the peri-
560 odic convective mixing events will have some small but
561 random effect on the overall magnetic field strength we
562 are able to qualitatively reproduce the increase activity
563 spread in a synthetic population of stars.

564 This work has made use of the NASA astrophysical
565 data system (ADS). We would like to thank Elisabeth
566 Newton, Aaron Dotter, and Gregory Feiden for their
567 support and for useful discussion related to the topic
568 of this paper. Additionally, we would like to thank
569 Keighley Rockcliffe, Kara Fagerstrom, and Isabel Hal-
570 stead for their useful discussion related to this work.
571 **Finally, we would like to thank the referee for**
572 **their careful reading and critique of this arti-**
573 **cle.** We acknowledge the support of a NASA grant (No.
574 80NSSC18K0634).

575 *Software:* The Dartmouth Stellar Evolution Program
576 (DSEP) (*Dotter et al. 2008*), *BeautifulSoup* (*Richardson*
577 *2007*), *mechanize* (*Chandra&Varanasi2015*), *FreeEOS* (*Ir-*
578 *win 2012*), *pyTOPSScrape* (*Boudreaux 2022*), *lightkurve*
579 (*Lightkurve Collaboration et al. 2018*), *stella* (*Feinstein*
580 *et al. 2020a*), *starspot* (*Angus 2021; Angus & Garcia Soto*
581 *2023*)

REFERENCES

582 Angus, R. 2021, Zenodo, doi: [10.5281/zenodo.4613887](https://doi.org/10.5281/zenodo.4613887)
583 Angus, R., & Garcia Soto, A. 2023,
584 *agarciasoto18/starrotate: Alternate Starrotate for Paper,*
585 *v1.1.1, Zenodo, doi: 10.5281/zenodo.7697238.*
586 <https://doi.org/10.5281/zenodo.7697238>
587 Angus, R., Morton, T., Aigrain, S., Foreman-Mackey, D., &
588 Rajpaul, V. 2018, *Monthly Notices of the Royal*
589 *Astronomical Society*, 474, 2094,
590 doi: [10.1093/mnras/stx2109](https://doi.org/10.1093/mnras/stx2109)
591 Astudillo-Defru, N., Delfosse, X., Bonfils, X., et al. 2017,
592 *A&A*, 600, A13, doi: [10.1051/0004-6361/201527078](https://doi.org/10.1051/0004-6361/201527078)
593 Baraffe, I., & Chabrier, G. 2018, *A&A*, 619, A177,
594 doi: [10.1051/0004-6361/201834062](https://doi.org/10.1051/0004-6361/201834062)
595 Barentsen, G., Hedges, C., Vinícius, Z., et al. 2020,
596 *KeplerGO/Lightkurve: Lightkurve v1.11.0, Zenodo,*
597 doi: [10.5281/zenodo.3836658](https://doi.org/10.5281/zenodo.3836658)
598 Boisse, I., Bouchy, F., Hébrard, G., et al. 2011, *A&A*, 528,
599 A4, doi: [10.1051/0004-6361/201014354](https://doi.org/10.1051/0004-6361/201014354)
600 Boudreaux, E. M., & Chaboyer, B. C. 2023, *ApJ*, 944, 129,
601 doi: [10.3847/1538-4357/acb685](https://doi.org/10.3847/1538-4357/acb685)
602 Boudreaux, E. M., Newton, E. R., Mondrik, N.,
603 Charbonneau, D., & Irwin, J. 2022, *ApJ*, 929, 80,
604 doi: [10.3847/1538-4357/ac5cbf](https://doi.org/10.3847/1538-4357/ac5cbf)

- 605 Boudreaux, T. 2022, `tboudreaux/pytopsscrape`:
606 `pyTOPSScrape v1.0`, v1.0, Zenodo,
607 doi: [10.5281/zenodo.7094198](https://doi.org/10.5281/zenodo.7094198).
608 <https://doi.org/10.5281/zenodo.7094198>
- 609 Chabrier, G., & Küker, M. 2006, *A&A*, 446, 1027,
610 doi: [10.1051/0004-6361:20042475](https://doi.org/10.1051/0004-6361:20042475)
- 611 Chandra, R. V., & Varanasi, B. S. 2015, *Python requests*
612 *essentials* (Packt Publishing Ltd)
- 613 Cretignier, M., Pietrow, A. G. M., & Aigrain, S. 2024,
614 *MNRAS*, 527, 2940, doi: [10.1093/mnras/stad3292](https://doi.org/10.1093/mnras/stad3292)
- 615 Curtis, J. L., Agüeros, M. A., Matt, S. P., et al. 2020, *ApJ*,
616 904, 140, doi: [10.3847/1538-4357/abf58](https://doi.org/10.3847/1538-4357/abf58)
- 617 Dotter, A., Chaboyer, B., Jevremović, D., et al. 2008, *The*
618 *Astrophysical Journal Supplement Series*, 178, 89
- 619 Dungee, R., van Saders, J., Gaidos, E., et al. 2022, *ApJ*,
620 938, 118, doi: [10.3847/1538-4357/ac90be](https://doi.org/10.3847/1538-4357/ac90be)
- 621 Feiden, G. A., Skidmore, K., & Jao, W.-C. 2021, *ApJ*, 907,
622 53, doi: [10.3847/1538-4357/abcc03](https://doi.org/10.3847/1538-4357/abcc03)
- 623 Feinstein, A., Montet, B., & Ansdell, M. 2020a, *J. Open*
624 *Source Softw.*, 5, 2347, doi: [10.21105/joss.02347](https://doi.org/10.21105/joss.02347)
- 625 Feinstein, A. D., Montet, B. T., Ansdell, M., et al. 2020b,
626 *Astron. J.*, 160, 219, doi: [10.3847/1538-3881/abac0a](https://doi.org/10.3847/1538-3881/abac0a)
- 627 Fuhrmeister, B., Czesla, S., Schmitt, J. H. M. M., et al.
628 2019, *A&A*, 623, A24, doi: [10.1051/0004-6361/201834483](https://doi.org/10.1051/0004-6361/201834483)
- 629 Gallet, F., Charbonnel, C., Amard, L., et al. 2017, *A&A*,
630 597, A14, doi: [10.1051/0004-6361/201629034](https://doi.org/10.1051/0004-6361/201629034)
- 631 García Soto, A., Newton, E. R., Douglas, S. T., Burrows,
632 A., & Kesseli, A. Y. 2023, *AJ*, 165, 192,
633 doi: [10.3847/1538-3881/acc2ba](https://doi.org/10.3847/1538-3881/acc2ba)
- 634 Grevesse, N., & Sauval, A. J. 1998, *SSRv*, 85, 161,
635 doi: [10.1023/A:1005161325181](https://doi.org/10.1023/A:1005161325181)
- 636 Houdebine, E. R., Mullan, D. J., Bercu, B., Paletou, F., &
637 Gebran, M. 2017, *ApJ*, 837, 96,
638 doi: [10.3847/1538-4357/aa5cad](https://doi.org/10.3847/1538-4357/aa5cad)
- 639 Irwin, A. W. 2012, *FreeEOS: Equation of State for stellar*
640 *interiors calculations*, *Astrophysics Source Code Library*,
641 record `ascl:1211.002`. <http://ascl.net/1211.002>
- 642 Jao, W.-C., & Feiden, G. A. 2020, *AJ*, 160, 102,
643 doi: [10.3847/1538-3881/aba192](https://doi.org/10.3847/1538-3881/aba192)
- 644 —. 2021, *Research Notes of the American Astronomical*
645 *Society*, 5, 124, doi: [10.3847/2515-5172/ac053a](https://doi.org/10.3847/2515-5172/ac053a)
- 646 Jao, W.-C., Henry, T. J., Gies, D. R., & Hambly, N. C.
647 2018, *ApJL*, 861, L11, doi: [10.3847/2041-8213/aacdf6](https://doi.org/10.3847/2041-8213/aacdf6)
- 648 Jao, W.-C., Henry, T. J., White, R. J., et al. 2023, *AJ*, 166,
649 63, doi: [10.3847/1538-3881/ace2bb](https://doi.org/10.3847/1538-3881/ace2bb)
- 650 Kislyakova, K. G., Noack, L., Johnstone, C. P., et al. 2017,
651 *Nature Astronomy*, 1, 878,
652 doi: [10.1038/s41550-017-0284-0](https://doi.org/10.1038/s41550-017-0284-0)
- 653 Kleeorin, N., Rogachevskii, I., Safiullin, N., Gershberg, R.,
654 & Porshnev, S. 2023, *MNRAS*, 526, 1601,
655 doi: [10.1093/mnras/stad2708](https://doi.org/10.1093/mnras/stad2708)
- 656 Kochukhov, O. 2021, *A&A Rv*, 29, 1,
657 doi: [10.1007/s00159-020-00130-3](https://doi.org/10.1007/s00159-020-00130-3)
- 658 Kumar, M., & Fares, R. 2023, *MNRAS*, 518, 3147,
659 doi: [10.1093/mnras/stac2766](https://doi.org/10.1093/mnras/stac2766)
- 660 Kumar, V., Rajpurohit, A. S., Srivastava, M. K.,
661 Fernández-Trincado, J. G., & Queiroz, A. B. A. 2023,
662 *MNRAS*, 524, 6085, doi: [10.1093/mnras/stad2222](https://doi.org/10.1093/mnras/stad2222)
- 663 Lammer, H., Güdel, M., Kulikov, Y., et al. 2012, *Earth*,
664 *Planets and Space*, 64, 179, doi: [10.5047/eps.2011.04.002](https://doi.org/10.5047/eps.2011.04.002)
- 665 Lightkurve Collaboration, Cardoso, J. V. d. M., Hedges, C.,
666 et al. 2018, *Astrophysics Source Code Library*,
667 `ascl:1812.013`
- 668 Mansfield, S., & Kroupa, P. 2021, *A&A*, 650, A184,
669 doi: [10.1051/0004-6361/202140536](https://doi.org/10.1051/0004-6361/202140536)
- 670 Middelkoop, F. 1982, *A&A*, 107, 31
- 671 Newton, E. R., Irwin, J., Charbonneau, D., et al. 2016,
672 *ApJ*, 821, 93, doi: [10.3847/0004-637X/821/2/93](https://doi.org/10.3847/0004-637X/821/2/93)
- 673 Nutzman, P., & Charbonneau, D. 2008, *PASP*, 120, 317,
674 doi: [10.1086/533420](https://doi.org/10.1086/533420)
- 675 Perdelwitz, V., Mittag, M., Tal-Or, L., et al. 2021, *VizieR*
676 *Online Data Catalog*, *J/A+A/652/A116*,
677 doi: [10.26093/cds/vizier.36520116](https://doi.org/10.26093/cds/vizier.36520116)
- 678 Rauscher, E., & Marcy, G. W. 2006, *PASP*, 118, 617,
679 doi: [10.1086/503021](https://doi.org/10.1086/503021)
- 680 Richardson, L. 2007, *April*
- 681 Robertson, P., Stefansson, G., Mahadevan, S., et al. 2020,
682 *ApJ*, 897, 125, doi: [10.3847/1538-4357/ab989f](https://doi.org/10.3847/1538-4357/ab989f)
- 683 Rodríguez-López, C. 2019, *Frontiers in Astronomy and*
684 *Space Sciences*, 6, 76, doi: [10.3389/fspas.2019.00076](https://doi.org/10.3389/fspas.2019.00076)
- 685 Rutten, R. G. M. 1984, *A&A*, 130, 353
- 686 Saar, S. H., & Linsky, J. L. 1985, *ApJL*, 299, L47,
687 doi: [10.1086/184578](https://doi.org/10.1086/184578)
- 688 Salvatier, J., Wiecki, T. V., & Fonnesbeck, C. 2016, *PeerJ*
689 *Comput. Sci.*, 2, e55, doi: [10.7717/peerj-cs.55](https://doi.org/10.7717/peerj-cs.55)
- 690 Shulyak, D., Sokoloff, D., Kitchatinov, L., & Moss, D. 2015,
691 *MNRAS*, 449, 3471, doi: [10.1093/mnras/stv585](https://doi.org/10.1093/mnras/stv585)
- 692 Shulyak, D., Reiners, A., Nagel, E., et al. 2019, *A&A*, 626,
693 A86, doi: [10.1051/0004-6361/201935315](https://doi.org/10.1051/0004-6361/201935315)
- 694 Skrutskie, M. F., Cutri, R. M., Stiening, R., et al. 2006, *AJ*,
695 131, 1163, doi: [10.1086/498708](https://doi.org/10.1086/498708)
- 696 Spada, F., & Lanzafame, A. C. 2020, *A&A*, 636, A76,
697 doi: [10.1051/0004-6361/201936384](https://doi.org/10.1051/0004-6361/201936384)
- 698 Vaughan, A. H., Baliunas, S. L., Middelkoop, F., et al.
699 1981, *ApJ*, 250, 276, doi: [10.1086/159372](https://doi.org/10.1086/159372)
- 700 Winters, J. G., Henry, T. J., Jao, W.-C., et al. 2019, *AJ*,
701 157, 216, doi: [10.3847/1538-3881/ab05dc](https://doi.org/10.3847/1538-3881/ab05dc)

702 Wright, N. J., Newton, E. R., Williams, P. K. G., Drake,
703 J. J., & Yadav, R. K. 2018, MNRAS, 479, 2351,
704 doi: [10.1093/mnras/sty1670](https://doi.org/10.1093/mnras/sty1670)